



Journal of Advanced Research in Fluid Mechanics and Thermal Sciences

Journal homepage:
https://semarakilmu.com.my/journals/index.php/fluid_mechanics_thermal_sciences/index
ISSN: 2289-7879



Integration of a Gamma-Type Stirling Engine with LPG Cooking Stove for Micro-Scale Combined Heat and Power Generation

Jufrizal^{1,2}, Farel Hasiholan Napitupulu^{1,*}, Ilmi¹, Himsar Ambarita¹, Supriatno², Muhammad Irwanto³

¹ Department of Mechanical Engineering, Faculty of Engineering, Universitas Sumatera Utara, 20155 Medan, Indonesia

² Department of Mechanical Engineering, Faculty of Engineering, Universitas Medan Area, 20223 Medan, Indonesia

³ Fellow of Center of Excellence for Renewable Energy, Universiti Malaysia Perlis, 02600 Arau Perlis, Malaysia

ARTICLE INFO

ABSTRACT

Article history:

Received 20 May 2023

Received in revised form 15 July 2023

Accepted 22 July 2023

Available online 11 August 2023

Keywords:

A customized cooking stove burner; combined heat and power; gamma type Stirling engine

The Stirling engine is one of the most versatile micro-scale prime movers for combined heat and power applications, adaptable to different levels of heat sources. This study started a unique journey that included developing, experimenting, and analyzing the Gamma-type Stirling engine. Notably, the engine design ingeniously harnesses heat from a customized cooking stove burner powered by liquefied petroleum gas. The engine fabrication resulted in a compression ratio 2.014, accommodating a volumetric capacity of 181 cc. The Stirling engine test used air as the working gas, and the initial conditions were at atmospheric pressure. Stirling engine performance was analyzed using an ideal thermodynamic cycle model and burner efficiency using the water boiling method. The modified burner attains an average temperature of 699.5°C, producing a burner power output of 5.702 kW and a thermal efficiency of 32.7% or around 1.867 kW of heat for operating the engine and cooking activities. Simultaneously, tests of the Stirling engine revealed an average air temperature difference of 146.2°C between the expansion and compression phases. The flywheel rotation speed ranges from 158 to 369 rpm. During testing, the Stirling engine obtained an average thermal efficiency of 31.08%, accompanied by an ideal power spectrum ranging from 0.3 W to 42.6 W. The highlight of this study was the maximum pressure achieved at the end of the heat absorption stage, recorded at 296.1 kPa. Importantly, these findings underscore the promising potential of micro-Combined Heat and Power systems. Integrating the gamma-type Stirling engine with the LPG stove represents novelty and paves the way for further development and advancement in sustainable energy solutions.

1. Introduction

Enhancing energy efficiency in thermal systems is vital for conserving energy and mitigating environmental concerns. Many efforts have been made by researchers to increase thermal efficiency, such as nanorefrigerant technology as a substitute for working fluids in refrigeration systems [1,2], improving the characteristics and properties of phase change materials in heat energy storage, modification of the Rankine system to an organic Rankine cycle, and combined heat and power (CHP)

* Corresponding author.

E-mail address: farel@usu.ac.id

<https://doi.org/10.37934/arfmts.108.2.116>

in the stove or furnace [3-6]. This article will examine implementing a CHP system at the house scale. CHP, or cogeneration, is a system that works together to produce heat and generate electricity using one fuel. CHP has proven beneficial for residential and industrial use due to its high overall thermal efficiency compared to the separate production of heat and electrical energy [7]. CHP technology can be applied to internal combustion, external combustion, and no-combustion processes according to the use scale [8]. CHP technology is usually developed according to the type of fuel used. Micro-scale CHP technology (mCHP) in external combustion cases usually uses a Stirling engine as the prime mover [9-12]. In much literature, the Stirling engine's main characteristics meet the requirements for mCHP applications due to long service life, long service intervals, high efficiency, low noise and vibration, and low emissions [13,14].

Stirling engines with various configurations for specific applications have not yet been commercially sold, such as gasoline and diesel engines. Hence, researchers need to design and manufacture them before testing. The Stirling engine has unique characteristics in its design and performance. Engine efficiency and performance are affected by external heat sources, engine configuration, material selection, temperature differences, heat characteristics, operating modes, charging pressures, physical, geometric features, and the type of working gas used [15-17]. The choice of working gas significantly impacts the efficiency and performance of the gamma-type Stirling engine. This working gas must be able to expand and compress as it moves through the thermal cycle. The thermal and physical characteristics of the active gas, such as heat capacity, viscosity, and thermal conductivity, will affect the thermal efficiency and the ability of the engine to convert heat to mechanical work. Stirling engines usually use air or gases, such as helium, hydrogen, nitrogen, and methanol, as the working fluid [18]. The development and optimization of the Stirling engine prototype with gamma configuration for various applications in various fields, such as power generation, cooling, and heating, have been investigated by researchers [19-22]. The development of the Gamma-type Stirling engine has also been extensively researched to utilize heat from various external heat sources. External heat sources commonly used to operate small-scale Stirling engines such as solar energy, liquefied petroleum gas (LPG), and biomass. A study on the efficiency of the Stirling engine using a parabolic mirror to focus solar radiation on the engine has been carried out [23]. Developing a beta-type Stirling engine for low and medium-temperature heat sources using heat input from domestic gas burners has also been carried out [24,25]. Stirling engine type LTD (low temperature differential) has also been tested using an LPG burner to see the effect of material displacers [25]. The utilization of a biomass-based low-level temperature heat source has been modeled, and the results show that the computational model can be used to evaluate the performance of a Stirling engine [26,27]. Besides being used separately with an external heat source, the Stirling engine can also be integrated with a wood pellet burner [28]. The development of a gamma-type Stirling engine for mCHP applications has also been carried out by the authors together with the team since 2017 until now which has resulted in two engine prototypes named mCPHSE-012018 and mCHPSE-012019 [29-31]. The two generations of Stirling engines that have been manufactured are shown in Figure 1. One of the causes the gamma configuration is more desirable to develop because it has a higher power output and thermal efficiency than alpha and beta [32,33].

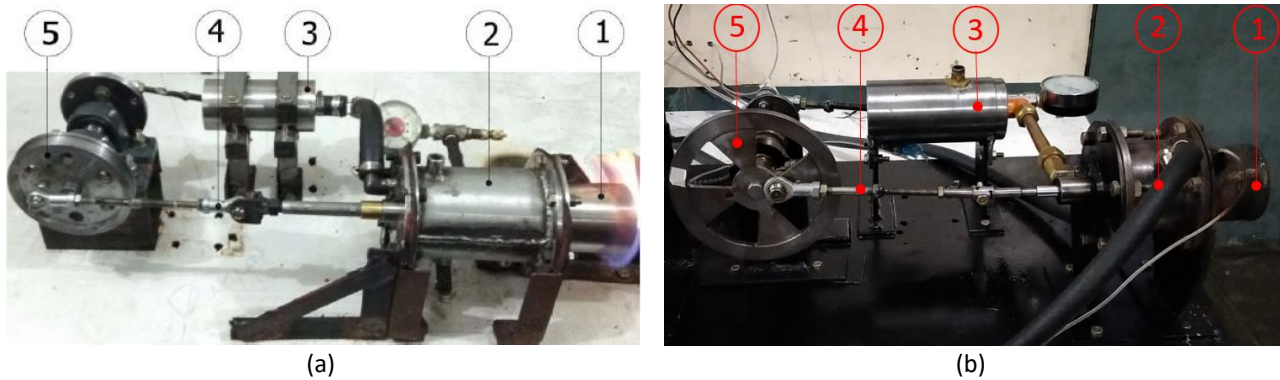


Fig. 1. Prototype Stirling engine type gamma (a) mCHPSE-012018 (b) mCHPSE-012019

Figure 1 shows the main components of the two Stirling engines, namely heater (1), displacer section (2), piston section (3), connecting rod (4), and flywheel (5). At the same time, the comparison of the parameters of the two Stirling engines from the results of thermodynamic calculations and analysis is shown in Table 1.

Table 1

Comparison of the specifications of the Gamma-type Stirling engine that has been manufactured

No.	Parameter	Unit	Value	
			mCHPSE-012018	mCHPSE-012019
1.	Working gas		air	air
2.	Starting engine pressure	bar	1.01325	1.01325
3.	Maximum volume	cc	338	201
4.	Minimum volume	cc	232	110
5.	Compression ratio		1.46	1.82
6.	Temperature difference	°C	74.7	132
7.	Maximum flywheel rotation speed	rpm	242.6	415
8.	Thermal efficiency	%	18.78	24.6
9.	Maximum pressure	bar	1.82	2.446
10.	Maximum power	W	12.9	37.9

Based on previous studies of the two previous designs, it was found that the performance of the Stirling engine is strongly related to the working gas temperature difference between the expansion and compression space. One factor affecting the working gas temperature difference is the external heat source. The component that plays a vital role in producing a heat source in this system is the burner. This component is also used in conventional LPG cooking stoves with the same function. Because the Stirling engine design is intended for mCHP applications utilizing heat sources from cooking activities, this burner component needs to be modified to be used together in this system, which functions for both processes, namely heating the working gas and cooking. The burner integration concept of the Stirling Engine with the cooking stove is the focus of this experimental research study because previous studies on the Stirling engine have not been carried out. This study aims to determine the performance of the Stirling engine mCHPSE-012020 using a heat source generated from an LPG burner integrated with a cooking stove. This research is crucial because the technological development outcomes are anticipated to support global initiatives to identify sustainable and environmentally friendly energy sources and improve energy efficiency in household applications.

2. Engine Construction and Analysis

2.1 Stirling Engine mCHPSE-012020

The third-generation gamma-type Stirling engine prototype began to be developed in 2020. The layout of the Stirling engine prototype has been developed and the burner is shown in Figure 2. One difference from the previous design is that the engine position changes from horizontal to vertical because the heater adjusts to the heat source from the cooking stove burner. The Stirling engine developed with the mCHPSE research team is named mCHPSE-012020. This engine consists of several main parts, namely the burner, heater, expansion space, connection pipe, compression space, and flywheel, whose design is shown in Figure 2.

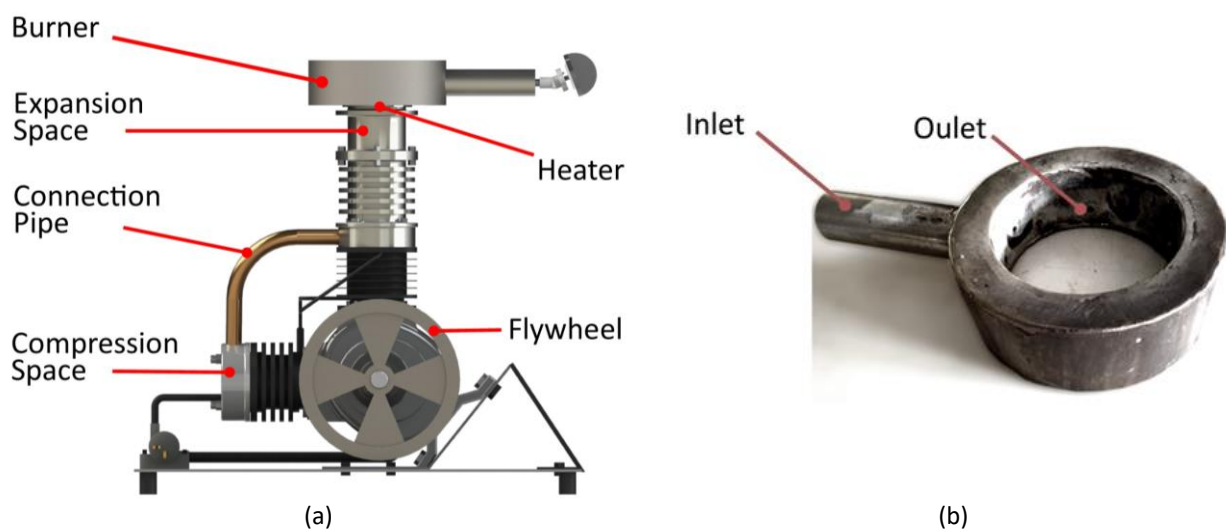


Fig. 2. (a) Layout prototype Stirling engine type gamma mCHPSE-012020 (b) Burner LPG modification

The burner is designed in the form of a ring to adjust the position of the heater, which is vertical. Besides heating the heater wall, the burner also functions as a cooking stove. The burner is made of Stainless Steel 304 material with a plate thickness of 2.5 mm, a burner height of 55 mm and a width of 22.5 mm. The length of the inlet pipe is 110 mm, with an inner diameter of 30 mm. The outer diameter of the burner is 140 mm, and the inside diameter is 105 mm, with the distance from the inner wall to the outer wall of the heater being 25 mm. Several burner holes are made of 16 pieces, and the outlet hole diameter is 4 mm. Additional components on the burner to function as a cooking stove are the pan support, flintstone (ignition system and gas system), and knob. Flintstone functions to extinguish the fire and regulate the gas output from the sprayer; the sprayer functions to spray and change the gas flow speed to faster and functions as a safety guard so that the fire does not return to the LPG gas cylinder. The pan support functions as a pot holder with a distance of 65 mm from the burner outlet. All of these additional components are taken from LPG stoves on the market with SNI standards (Indonesian national standards). In addition, a blower is also added, which functions to supply additional air to the burner so that the combustion process improves.

The heater is one of the important components of the Stirling engine, which heat the working gas in the cylinder so that the gas expands and pushes the piston or displacer to produce mechanical motion. Heaters are typically constructed from materials with high thermal conductivity, like copper, aluminum, and stainless steel. Heaters can be in the form of pipes, plates, and coils that are placed near an external heat source. The heater used in this Stirling engine is in the form of a pipe manufactured using stainless steel. Stainless steel was chosen as a Stirling engine heater material because it has high thermal conductivity, oxidation and corrosion resistance, mechanical strength,

and low availability and cost compared to other materials such as copper, aluminum, or ceramics. The heater has an outer diameter of 55 mm, a height of 90 mm, and a thickness of 5 mm on each wall.

The next main component is the expansion space, which is a space where the working gas undergoes isothermal expansion when heated by an external heat source. The expansion space is also connected to the displacer, which moves the working gas from the hot room to the cold room or vice versa. The expansion space in this design is connected to the compression space via a connection pipe. The connection pipe on the Stirling engine flows the working gas from the compression chamber to the expansion chamber or vice versa, as well as to exchange heat between the working gas and the cooler. Compression space is in the engine cylinder where air or working gas is compressed. The Gamma-type Stirling engine separates the displacer and the power piston cylinders. The compression chamber is inside the power piston cylinder, while the displacer cylinder is in moving air or working gas between the hot and cold sources. The last major component is the flywheel mounted on the crankshaft to store kinetic energy from engine rotation and reduce rotational speed fluctuations. In addition, the flywheel also maintains the engine's angular momentum and generates constant torque. The specifications of the main parts of the Stirling mCHPSE-012020 engine that have been designed and manufactured are shown in Table 2.

Table 2
 Main component sizes of the Stirling engine mCHPSE-012020

B_{dp} (mm)	S_{dp} (mm)	B_{pp} (mm)	S_{pp} (mm)	B_{cp} (mm)	S_{cp} (mm)	S_{DE} (mm)	S_{DC} (mm)	α (deg)	j (deg)
45	45	50.75	45	8	290	1	1	0-360	90

Table 2 shows the main dimensions of the Stirling engine mCHPSE-012020, including the displacer cylinder diameter, B_{dp} ; displacer piston stroke length, S_{dp} ; power piston cylinder diameter, B_{pp} ; power piston stroke length, S_{pp} ; connection pipe diameter, B_{cp} ; connection pipe length, S_{cp} ; dead volume length of expansion space, S_{DE} ; dead volume length of compression space, S_{DC} ; crank angle, α and phase angle, φ .

2.2 Analysis of Stirling Engine

Researchers have developed many methods for analyzing the Stirling engine. Some of these models include the ideal adiabatic model, ideal polytropic analysis, Urieli and Berchowitz model (simple analysis), simple polytropic analysis, Timoumi model, simple-II model, Polytropic analysis of Stirling engine with various loss mechanisms (PSVL) approach, The combined adiabatic-finite speed thermal approach (CAFS) model, finite speed thermodynamic analysis, developed analytical isothermal model, third order analysis, and modified PSVL [34]. In this paper, the analysis used is the ideal cycle model. The author and other researchers in previous papers have discussed the ideal cycle model used in this investigation [31,35]. The selection of the ideal cycle model in this paper is due to the initial research, conceptual design, and focus on the basic characteristics of the Stirling engine. The ideal cycle model is also a simple approach to modeling basic thermodynamic processes to provide a good understanding of basic performance. The thermal efficiency, η_{th} , and work, P (W), produced at the ideal Stirling cycle can be calculated by Eq. (1) and Eq. (2).

$$\eta_{th} = 1 - \frac{T_{min}}{T_{max}} = 1 - \frac{T_C}{T_E} \quad (1)$$

$$P = n \times W \quad (2)$$

where, T_{min} or T_c ($^{\circ}\text{C}$) is the compression space temperature, and T_{max} or T_E ($^{\circ}\text{C}$) is the expansion space temperature. n (rpm) is the rotational speed of the Stirling engine, and W (J) is the net work done by the cycle.

2.3 Analysis of LPG Burner

In this paper, the burner analysis that will be carried out includes the burner power and thermal efficiency of LPG burners. LPG power and burners were tested using the water boiling method. Burner power (kW), P_b , is the energy produced by the burner during the test time and is calculated by Eq. (3) [37].

$$P_b = \frac{m_f \times LHV_f}{t} \quad (3)$$

where m_f is the mass amount of LPG used during the test (kg), LHV_f is the lower calorific value of LPG fuel (kJ/kg), and t is the test time (s). The LPG fuel used is a product from PT Pertamina with the ELPIJI brand. The LHV_f of this LPG is reported to be 48,800 kJ/kg [37].

Thermal efficiency measures the degree to which an engine can convert fuel energy into useful energy or mechanical work. In this case, the LPG burner's efficiency is the ratio between the heat required to heat the air in the heater wall and boil the water in the pot compared to the heat generated from burning LPG gas. The equation used is a modified equation that is often used to calculate the burner efficiency of LPG gas stoves [38]. Mathematically it can be written as in Eq. (4).

$$\eta_b = \frac{[4.186(T_{wb}-T_{wi})(m_{v+w}-m_v)+2,260.m_{wg}]+[cp_a(T_{af}-T_{ai})(m_{h+a}-m_h)]}{m_f \times LHV_f} \times 100 \quad (4)$$

where, T_{wb} and T_{wi} is boiling and initial temperature of water ($^{\circ}\text{C}$), m_{v+w} and m_v is mass of pot plus water and mass of empty pot before test (kg), and m_{wg} is water vaporized (kg). 4.186 kJ/kg $^{\circ}\text{C}$ is the specific heat of water and 2,260 kJ/kg is the latent heat of vaporization for water [39]. cp_a is the specific heat of air (kJ/kg. $^{\circ}\text{C}$), T_{af} and T_{ai} is the final and initial temperature of air, and m_{h+a} and m_h is mass of heater plus air and mass of empty heater before test (kg).

3. Methodology

An overview of the Stirling engine test mCHPSE-012020, which is integrated with the LPG-fired cooking stove that has been produced, is shown in Figure 3. The scheme shows some equipment and instrumentation to measure variables in this study. The main equipment used is the Stirling engine mCHPSE-012020 with a burner which also functions as a cooking stove. The working gas from the Stirling engine uses ambient air. Measurement and recording of temperature data at each point, as shown in Figure 3, uses a temperature meter data logger with brand Anbai AT4208 with an accuracy of $0.2^{\circ}\text{C} \pm 2$ digits and has eight channels. The sensor is a K-type thermocouple with a temperature range of -200°C to 1300°C . The temperature measured includes water in the pot (T_w), heat source (T_s), expansion space (T_E), cooling water (T_{cw}), and compression space (T_c). The measurement of the flywheel rotational speed, using a pulse meter Autonics MP5Y 4N and Autonics PR12-4DN proximity sensor. Measurement of the mass of LPG fuel, m_f , before and after testing using a Smart brand digital scale with a capacity of 30 kg. The fuel used is LPG with a 3 kg tank packaging commonly used for

cooking in Indonesia. LPG gas's maximum mass and pressure in the tank are around 5 kg and 800 kPa (8 bar).

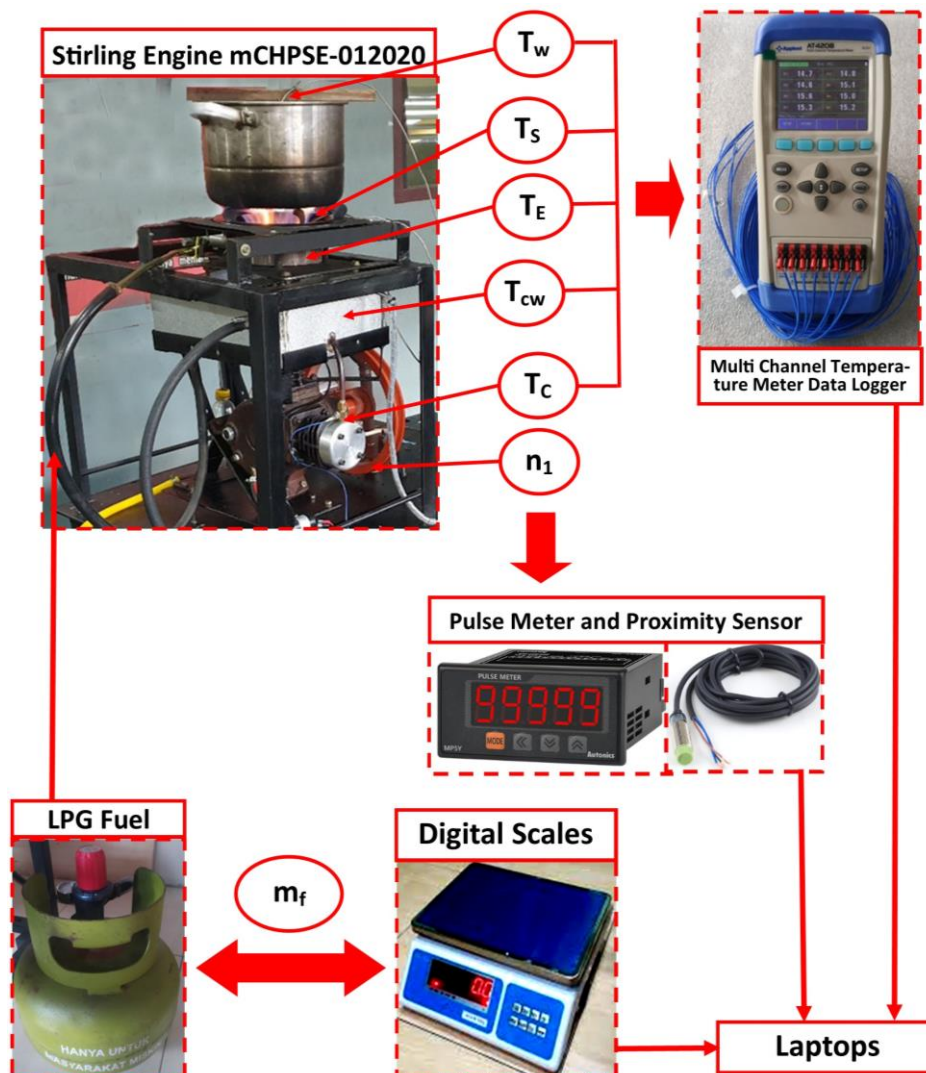


Fig. 3. Schematic layout of the experimental setup

The water boiling method was used to test the Stirling engine mCHPSE-012020 and the LPG cooking stove. The amount of water used is 2/3 of the volume of the pot, on a mass basis of 9.347 kg. The volume flow rate of LPG fuel and airflow rate is controlled at 0.0028 m³/minute and two m/second. The test was carried out for 3 hours (180 minutes) with data recording intervals every 1 minute for the temperature and flywheel rotating speed. The test results data obtained were then calculated and analyzed using Microsoft Excel software.

4. Results and Discussion

4.1 LPG Burner Efficiency and Performance

The mass of LPG fuel before and after testing from the measurement results obtained 7.537 kg and 6.275 kg, so the consumption of LPG fuel is around 1.262 kg for 180 minutes or the equivalent of 0.000117 kg/s. After calculating using Eq. (1) and Eq. (2), the LPG burner power is 5.702 kW, and the thermal efficiency reaches 32.7%. This value illustrates the percentage of fuel energy successfully converted into useful work for both driving the Stirling engine and cooking stove activities. The more

effectively the system consumes fuel, the higher the thermal efficiency. The efficiency value obtained shows that it is still low compared to the efficiency of LPG gas stoves on the market, namely $51 \pm 6\%$ [40]. Therefore, it is necessary to investigate which factors are most dominant to increase burner thermal efficiency and reduce fuel consumption so that they can become inputs for future burner designs. As it is known that the ability of LPG burners is influenced by factors such as burner design, combustion settings, environmental conditions, and the quality of the LPG used.

4.2 Volumes as a Function of the Crank Angle

Stirling engine volume, in general, can be affected by several factors, including crank angle. If the data from the measurement and calculation of the volume of the Stirling mCHPSE-012020 engine is plotted in graphical form, it is shown in Figure 4. The graph shows that the total volume at maximum conditions occurs at the crank angle position between 265° to 275° , which is around 0.000181 m^3 (181 cc) and minimum crank angle position between 80° to 100° with a value of about 0.000090 m^3 (90 cc). Figure 4 also shows that the maximum volume in the expansion chamber occurs at a crank angle position of 180° which is 0.0000716 m^3 (71.6 cc), and for the compression space, it occurs at a crank angle position of 310° which is 0.0001392 m^3 (139.2 cc).

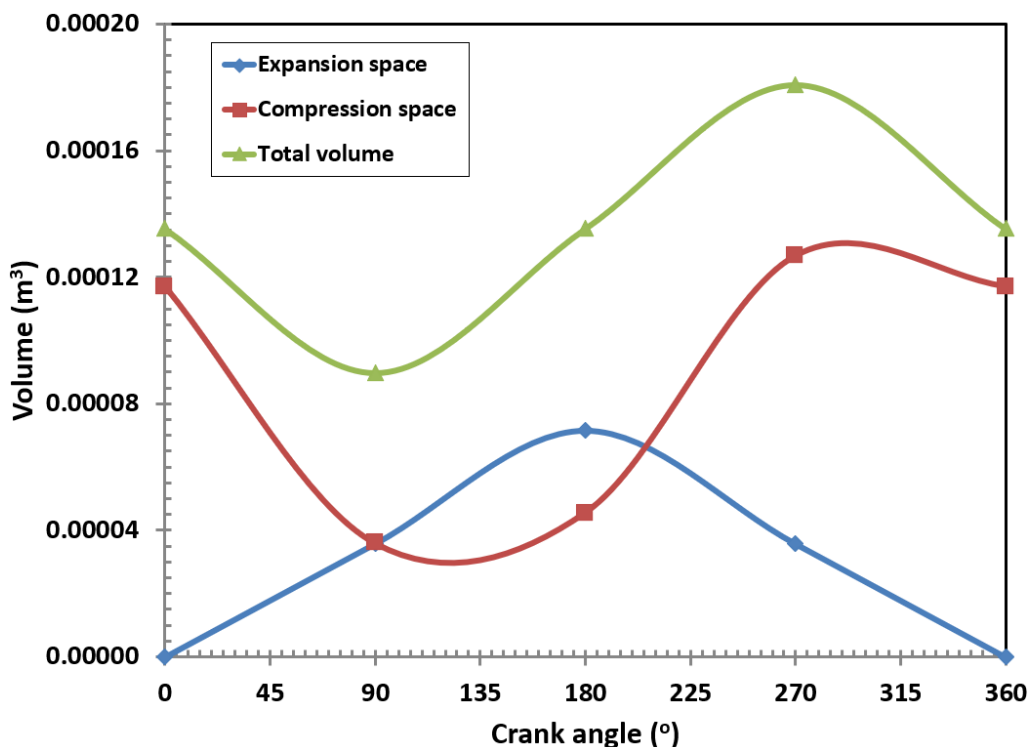


Fig. 4. Volume as a function of the crank angle for the Stirling engine

Although crank angle plays a role in the working cycle of a Stirling engine, engine volume also depends on other variables such as pressure, temperature and the overall system thermal characteristics. Figure 4 also shows the change in volume of the two main space containing working gas, namely the expansion space (hot space) and compression space (cold space). When the working gas is heated in the hot chamber, the gas pressure increases and the gas expands, causing a volume change. At the same time, the working gas in the cold room becomes colder, the gas pressure decreases, the gas contracts, and the volume change also occurs.

4.3 Engine Temperature and Speed

The Stirling engine mCHPSE-012020 test has been carried out to measure the temperature and engine speed. The temperature of the engine parts from the test results is shown in Figure 5. The temperature of the heat source from the combustion results uses LPG fuel and a modified burner. This temperature seems to be close to stable in the 10th minute because there is a preheater at the beginning of the process. The heat source temperature shows how much heat enters the Stirling engine. The average value of the heat source temperature is 699.5°C, which is high enough to produce a large working gas pressure. The maximum value is 713.1°C, which indicates that the heat source used is quite stable and not too volatile. The expansion chamber temperature shows how much heat the working gas absorbs in the hot cylinder. The average temperature of the expansion chamber is 197.2°C, which is quite low compared to the temperature of the heat source. It is shown that heat loss occurs between the heat source and the hot cylinder. The maximum value is 220.9°C, which indicates that there are variations in the temperature of the expansion space, which are influenced by other factors, such as the working gas flow rate, piston displacer vibration frequency, and thermal insulation.

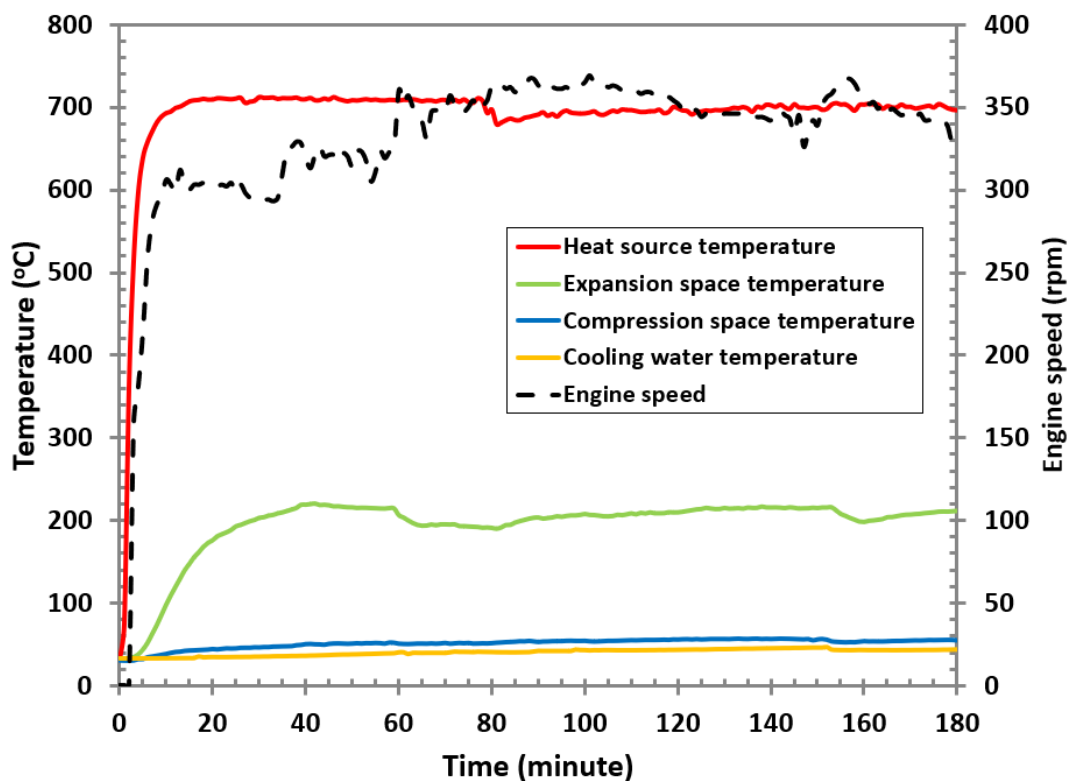


Fig. 5. Data on the results of testing the temperature and rotational speed of the Stirling engine flywheel mCHPSE-012020

The compression chamber temperature shows how much heat the working gas releases in the cold cylinder. The average value of the compression chamber temperature is 51°C, which is quite low compared to the expansion chamber temperature. It is indicated that there is effective heat transfer between the cold cylinder and the cooling water. The maximum value is 56.2°C, which indicates variations in the compression chamber temperature are influenced by other factors such as the expansion section. The cooling water temperature shows how much heat the cooling water from the cold cylinder absorbs. The average value of cooling water temperature is 40.4°C, which is quite low

for cooling water. It is shown that the cooling water is quite effective in cooling the air before entering the compression chamber. The maximum value is 47°C, which indicates variations in cooling water temperature which are influenced by other factors, such as cooling water flow rate, cooling water tank capacity, and ambient temperature.

The flywheel rotational speed of the Stirling engine during the test is shown in Figure 5 on the second y-axis. The engine flywheel rotational speed indicates how fast the Stirling engine is operating. The Stirling engine started moving in the 3rd minute after the test with a rotational speed of 158 rpm. The average value of the engine flywheel rotating speed is 335.9 rpm, which is quite high for a Gamma-type Stirling engine. The maximum value is 369 rpm, which indicates that the Stirling engine can achieve optimal performance under certain conditions. The rotating speed of the Gamma-type Stirling engine flywheel is affected by the working gas pressure and the torque of the power piston. Power piston torque, which determines how much force is exerted by the power piston on the crankshaft. The greater the torque of the power piston, the greater the moment of force applied, and the faster the crankshaft rotates. The working gas pressure, the compression cylinder diameter, and the distance between the crankshaft fulcrum and the mean cylinder center affect the power piston torque.

4.4 Analysis of Engines Using the Ideal Cycle Model

Based on the data from previous measurements and calculations, to facilitate further calculations, a simple calculator was developed to calculate the performance of a gamma-type Stirling engine using an ideal thermodynamic cycle approach. This calculator was built with the help of Microsoft Excel 2019 with three conditions of temperature variation and engine rotation speed: minimum, maximum and average. The analysis of the calculations that have been carried out is shown in Figure 6. In the Stirling engine ideal cycle calculation shown in Figure 6, several important parameters are used to analyze engine performance. The required input parameters in the Stirling engine ideal cycle analysis are expansion and compression temperature (T_E and T_C), engine rotational speed (n), minimum and maximum volume (V_{max} and V_{min}), working gas preload pressure (p_1), and initial temperature of working gas (T_i). While the output parameters include the difference in air temperature between the expansion and compression space, ΔT ; thermal efficiency, η_{th} ; compression ratio, ε ; air masses at initial conditions, m_a ; the amount of heat energy absorbed by the air in the expansion and compression space, Q_E and Q_C ; work done by the system, W_{net} ; Stirling engine ideal power, P ; and pressures in states 2 to 4, p_2 , p_3 , and p_4 .

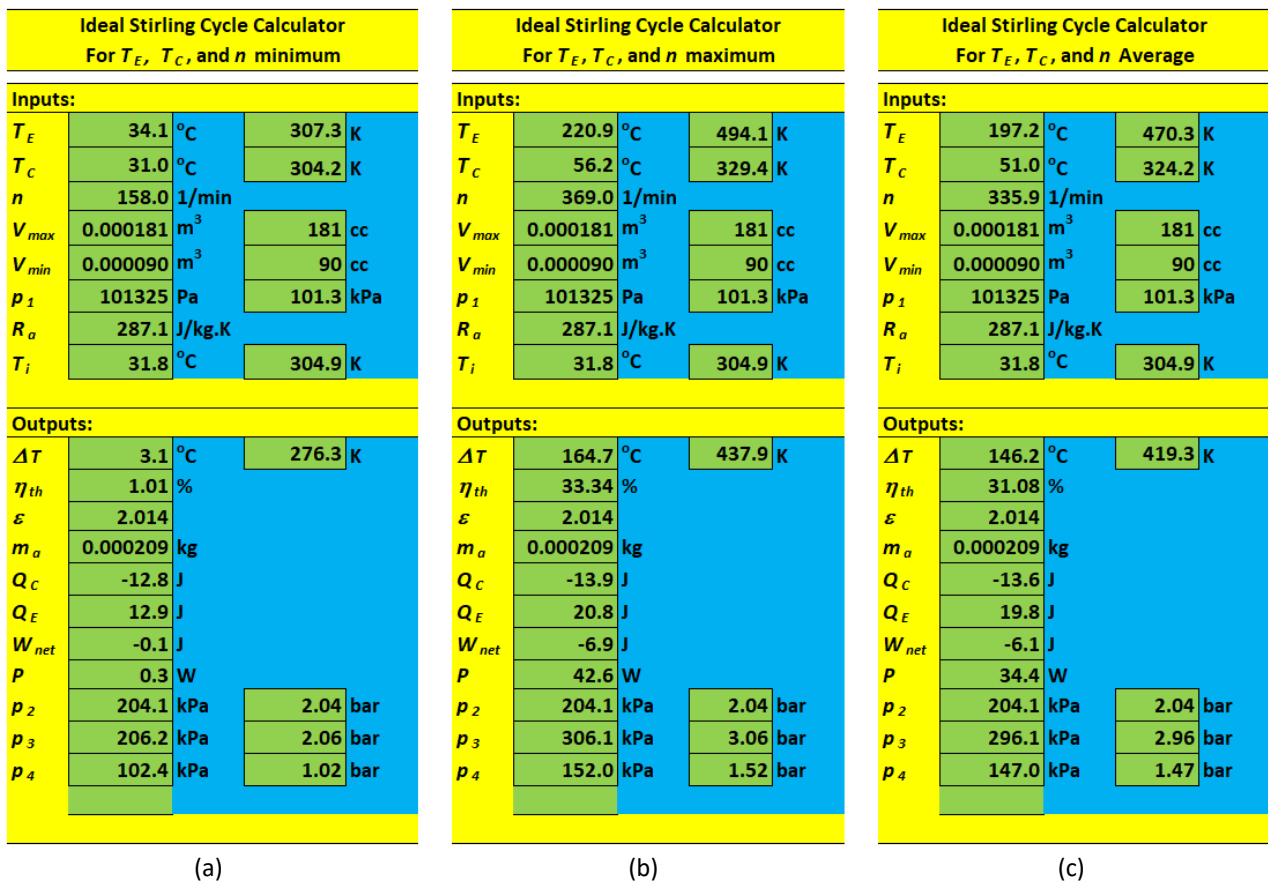


Fig. 6. Results of analysis using the Ideal Stirling cycle model (a) Minimum T_E , T_C , and n values (b) Maximum T_E , T_C , and n values (c) Average T_E , T_C , and n values

4.4.1 Temperature difference and thermal efficiency

Thermal efficiency is greatly affected by the temperature difference between the expansion and compression space. After data analysis, the difference between the minimum, maximum and average temperatures is 3.1°C, 164.7°C and 146.2°C. While the minimum, maximum and average thermal efficiency during successive tests were 1.01%, 33.34%, and 31.08%. It is shown that the greater the difference in air temperature between the expansion and compression space, the greater the thermal efficiency that the engine can achieve. If the relationship between these two parameters, in graphical form, is shown in Figure 7. If the relationship between the two variables in Figure 7 is made into the 6th-order polynomial regression equation as follows:

$$y = 7.2397E-12x^6 - 3.2895E-09x^5 + 5.4209E-07x^4 - 3.7628E-05x^3 + 2.1778E-04x^2 + 3.0995E-01x + 4.1487E-02 \quad (5)$$

This equation has a coefficient of determination (R^2) = 0.999452, which means that the regression model can explain around 99.9452% of the data variability, indicating that the model is very good at explaining the relationship between the variables involved. It is indicated that the equation is very suitable for describing patterns or trends in data.

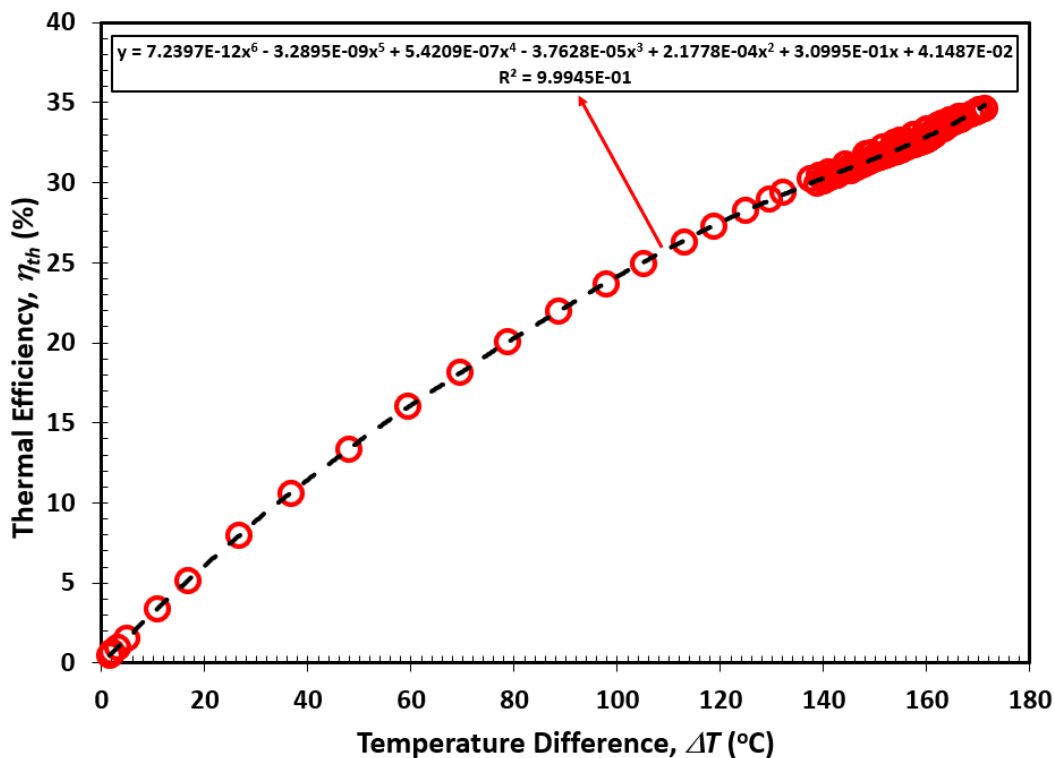


Fig. 7. The relationship between temperature difference and thermal efficiency in the Stirling engine mCHP2020

4.4.2 Compression ratio

The compression ratio of the Stirling engine can affect its performance and power output [16,41]. The compression ratio of the Stirling engine is the ratio between the maximum and minimum volumes of the working gas in the cycle. So based on the calculation results, it is obtained that the compression ratio is 2.014. The compression ratio obtained with the total dead volume of the Stirling mCHPSE-012020 engine is 0.00001819 m³ (18.19 cc). This Dead volume value is smaller than several other studies, which ranges from 169 cc to 250 cc [15,41].

4.4.3 Heat, work, and power of the ideal Stirling cycle

Figure 6 shows the calculation results of heat, work and power of the Stirling engine mCHPSE-012020 with three variations of input parameter conditions, namely minimum, maximum and average. The results of these calculations provide information about the performance of the Stirling engine in several conditions during its working cycle. When the minimum parameter shows that the heat difference between the compression and expansion space is relatively small, which causes the work produced to be relatively small (-0.1 J). The engine speed at this state is 158 rpm. The resulting output power is also low, only 0.3 W. At the maximum state, there is a more significant heat difference between the compression and expansion space which causes the work to be more meaningful (-6.9 J). The engine speed at this state is 369 rpm. The output power generated in this state increases relatively high, reaching 42.6 W. The average condition describes the average situation during the Stirling engine work cycle. The heat difference between the compression and expansion space at this state is between the minimum and maximum conditions. The work generated is lower than the maximum parameter (-6.1 J). The engine speed at this state is 335.9 rpm. The output power generated on average is 34.4 W. The difference in heat between the compression and

expansion space affects the amount of work generated and the output power of the Stirling engine. The greater the heat difference, the higher the work done by the system and output power. Engine speed also plays a vital role in the performance of the Stirling engine.

4.4.4 *p-V diagram of the ideal process*

The relationship between changes in working gas volume and pressure in the Stirling engine mCHPSE-012020 is based on a thermodynamic cycle in a closed system under conditions of average T_E , T_C , and n values, as shown in Figure 8. The Stirling cycle consists of four processes in different situations in the Stirling engine, characterized by volume, temperature, and pressure changes. The volume in states 1 and 4 (maximum volume) is 0.000181 m^3 . The volume in states 2 and 3 (minimum volume) is 0.000090 m^3 . The temperature in states 1 and 2 (maximum temperature) is 197.2°C . The temperature in states 3 and 4 (minimum temperature) is 51°C . The pressures in states 1, 2, 3, and 4 were 101.3 kPa, 204.1 kPa, 296.1 kPa, and 147 kPa, respectively. Changes in volume and pressure at the Stirling cycle allow the conversion of heat energy into mechanical energy. The working gas pressure determines how much force the active gas exerts on the power piston. The greater the operating gas pressure, the greater the force exerted, and the faster the power piston moves. The working gas pressure is affected by the temperature of the heat source, dead volume, and the type of working gas used.

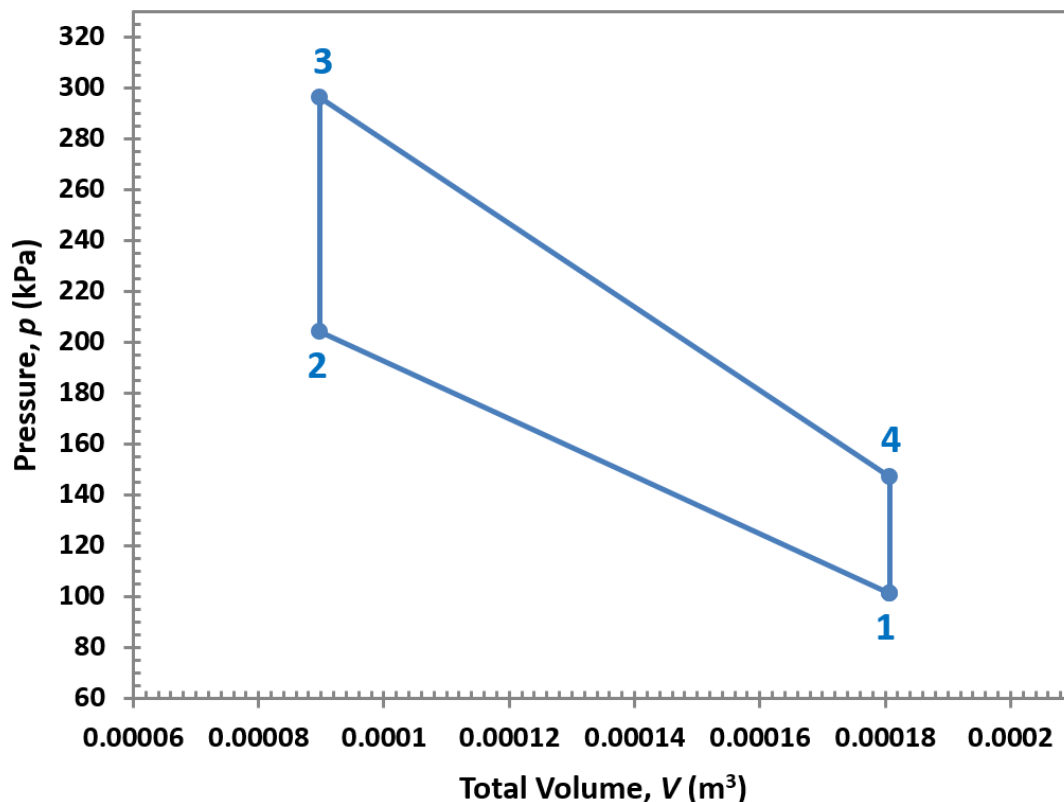


Fig. 8. Ideal Stirling cycle p-V diagram on T_E , T_C , and n average conditions

5. Conclusions

In this study, a Gamma-type Stirling engine called mCHPSE-012020 was used to convert heat energy from cooking activities into mechanical energy. Experimental studies show that the Stirling engine can convert most heat energy from cooking activity into mechanical energy. The Stirling

engine's performance in converting heat energy into mechanical energy has been evaluated. The results show that this engine can operate well and produce mechanical power but is still low, so it is necessary to optimize the design of each engine component to increase the power and rotational speed of the flywheel. This study opens up the potential for using a gamma-type Stirling engine as an energy utilization from cooking activities in the household. In the future, more research and development will need to be carried out to overcome the existing challenges and fully exploit the potential of this technology.

Acknowledgement

The authors would like to acknowledge the financial support from the Directorate General of Higher Education for financial support for the BPPDN scholarship that has been provided, the National Research and Innovation Agency for research assistance, and internal funding of the Universitas Medan Area Foundation in 2023. The authors also thank Mr Riclon H Sidabutar and Stirling Engine Research Team in 2020 at the Institut Teknologi Medan.

References

- [1] Halim, Nur Fazlin Che, and Nor Azwadi Che Sidik. "Mixing Chamber for Preparation of Nanorefrigerant." *Journal of Advanced Research in Applied Sciences and Engineering Technology* 21, no. 1 (2020): 32-40. <https://doi.org/10.37934/araset.21.1.3240>
- [2] Halim, Nur Fazlin Che, and Nor Azwadi Che Sidik. "Nanorefrigerants: A Review on Thermophysical Properties and Their Heat Transfer Performance." *Journal of Advanced Research in Applied Sciences and Engineering Technology* 20, no. 1 (2020): 42-50. <https://doi.org/10.37934/araset.20.1.4250>
- [3] Azmi, Mohd Irwan Mohd, Nor Azwadi Che Sidik, Yutaka Asako, Wan Mohd Arif Aziz Japar, Nura Muaz Muhammad, and Nadlene Razali. "Numerical Studies on PCM Phase Change Performance in Bricks for Energy-Efficient Building Application-A Review." *Journal of Advanced Research in Numerical Heat Transfer* 1, no. 1 (2020): 13-21.
- [4] Kean, Tung Hao, and Nor Azwadi Che Sidik. "Thermal performance analysis of nanoparticles enhanced phase change material (NEPCM) in cold thermal energy storage (CTES)." *CFD Letters* 11, no. 4 (2019): 79-91.
- [5] Ismail, H., A. A. Aziz, R. A. Rasih, N. Jenal, Z. Michael, and Azmi Roslan. "Performance of organic Rankine cycle using biomass as source of fuel." *Journal of Advanced Research in Applied Sciences and Engineering Technology* 4, no. 1 (2016): 29-46.
- [6] Schneider, T., D. Müller, and J. Karl. "A review of thermochemical biomass conversion combined with Stirling engines for the small-scale cogeneration of heat and power." *Renewable and Sustainable Energy Reviews* 134 (2020): 110288. <https://doi.org/10.1016/j.rser.2020.110288>
- [7] Noussan, Michel, Matteo Jarre, Roberta Roberto, and Daniele Russolillo. "Combined vs separate heat and power production-primary energy comparison in high renewable share contexts." *Applied Energy* 213 (2018): 1-10. <https://doi.org/10.1016/j.apenergy.2018.01.026>
- [8] Martinez, Simon, Ghislain Michaux, Patrick Salagnac, and Jean-Louis Bouvier. "Micro-combined heat and power systems (micro-CHP) based on renewable energy sources." *Energy Conversion and Management* 154 (2017): 262-285. <https://doi.org/10.1016/j.enconman.2017.10.035>
- [9] Borisov, Igor, Artem Khalatov, and Denis Paschenko. "The biomass fueled micro-scale CHP unit with stirling engine and two-stage vortex combustion chamber." *Heat and Mass Transfer* 58, no. 7 (2022): 1091-1103. <https://doi.org/10.1007/s00231-021-03165-z>
- [10] Najafi, Gholam, S. S. Hoseini, L. P. H. De Goey, and Talal Yusaf. "Optimization of combustion in micro combined heat and power (mCHP) system with the biomass-Stirling engine using SiO₂ and Al₂O₃ nanofluids." *Applied Thermal Engineering* 169 (2020): 114936. <https://doi.org/10.1016/j.applthermaleng.2020.114936>
- [11] Cardozo, Evelyn, and Anders Malmquist. "Performance comparison between the use of wood and sugarcane bagasse pellets in a Stirling engine micro-CHP system." *Applied Thermal Engineering* 159 (2019): 113945. <https://doi.org/10.1016/j.applthermaleng.2019.113945>
- [12] Qiu, Songgang, Yuan Gao, Garrett Rinker, and Koji Yanaga. "Development of an advanced free-piston Stirling engine for micro combined heating and power application." *Applied Energy* 235 (2019): 987-1000. <https://doi.org/10.1016/j.apenergy.2018.11.036>

- [13] Stamford, Laurence, Benjamin Greening, and Adisa Azapagic. "Life cycle environmental and economic sustainability of Stirling engine micro-CHP systems." *Energy Technology* 6, no. 6 (2018): 1119-1138. <https://doi.org/10.1002/ente.201700854>
- [14] Kaldehi, Bahare Jahani, Ali Keshavarz, Amir Ali Safaei Pirooz, Alireza Batooei, and Masood Ebrahimi. "Designing a micro Stirling engine for cleaner production of combined cooling heating and power in residential sector of different climates." *Journal of Cleaner Production* 154 (2017): 502-516. <https://doi.org/10.1016/j.jclepro.2017.04.006>
- [15] Cinar, Can, and Halit Karabulut. "Manufacturing and testing of a gamma type Stirling engine." *Renewable Energy* 30, no. 1 (2005): 57-66. <https://doi.org/10.1016/j.renene.2004.04.007>
- [16] Sowale, Ayodeji, Athanasios J. Kolios, Beatriz Fidalgo, Tosin Somorin, Alison Parker, Leon Williams, Matt Collins, Ewan McAdam, and Sean Tyrrel. "Thermodynamic analysis of a gamma type Stirling engine in an energy recovery system." *Energy Conversion and Management* 165 (2018): 528-540. <https://doi.org/10.1016/j.enconman.2018.03.085>
- [17] Joseph, Jerald, Erwin Mathew Louis, Befin Thomas, K. Anurag, Vishnu Sankar, and Thankachan T. Pullan. "Fabrication and testing of a gamma type stirling engine." *Materials Today: Proceedings* 46 (2021): 9641-9645. <https://doi.org/10.1016/j.matpr.2020.07.152>
- [18] Vahid, Davood Jalali, and Hojjat Danandeh Oskouei. "Design and anylisis of gamma type Stirling engine." *Mechanics & Industry* 21, no. 5 (2020): 511. <https://doi.org/10.1051/meca/2020062>
- [19] Khanjanpour, Mohammad Hassan, Mohammad Rahnema, Akbar A. Javadi, Mohammad Akrami, Ali Reza Tavakolpour-Saleh, and Masoud Iranmanesh. "An experimental study of a gamma-type MTD stirling engine." *Case Studies in Thermal Engineering* 24 (2021): 100871. <https://doi.org/10.1016/j.csite.2021.100871>
- [20] Topgül, Tolga, Melih Okur, Fatih Şahin, and Can Çınar. "Experimental investigation of the effects of hot-end and cold-end connection on the performance of a gamma type Stirling engine." *Engineering Science and Technology, an International Journal* 36 (2022): 101152. <https://doi.org/10.1016/j.jestch.2022.101152>
- [21] Daneshgar, Sareh, Rahim Zahedi, and Hamidreza Asemi. "Experimental investigation of gamma stirling engine coupling to convert thermal to cooling energy in different laboratory conditions." *Global Journal of Biotechnology and Biomaterial Science* 8, no. 1 (2022): 009-022. <https://doi.org/10.17352/gjibbs.000017>
- [22] Asemi, Hamidreza, Sareh Daneshgar, and Rahim Zahedi. "Experimental investigation of gamma Stirling refrigerator to convert thermal to cooling energy utilizing different gases." *Future Technology* 2, no. 2 (2023): 1-10. <https://doi.org/10.55670/fpll.futech.2.2.1>
- [23] Taki, Oumaima, Kaoutar Senhaji Rhazi, and Youssef Mejdoub. "A study of stirling engine efficiency combined with solar energy." *Advances in Science, Technology and Engineering Systems Journal* 6, no. 2 (2021): 837-45. <https://doi.org/10.25046/aj060297>
- [24] Karabulut, Halit, Hüseyin Serdar Yücesu, Can Çınar, and Fatih Aksoy. "An experimental study on the development of a β -type Stirling engine for low and moderate temperature heat sources." *Applied Energy* 86, no. 1 (2009): 68-73. <https://doi.org/10.1016/j.apenergy.2008.04.003>
- [25] Karabulut, H., C. Çınar, E. Oztürk, and H. S. Yücesu. "Torque and power characteristics of a helium charged Stirling engine with a lever controlled displacer driving mechanism." *Renewable Energy* 35, no. 1 (2010): 138-143. <https://doi.org/10.1016/j.renene.2009.04.023>
- [26] Rahman, Nik Kechik Mujahidah Nik Abdul, Syamimi Saadon, and Mohd Hasrizam Che Man. "Waste Heat Recovery of Biomass Based Industrial Boilers by Using Stirling Engine." *Journal of Advanced Research in Fluid Mechanics and Thermal Sciences* 89, no. 1 (2022): 1-12. <https://doi.org/10.37934/arfmts.89.1.112>
- [27] Rahman, Nik Kechik Mujahidah Nik Abdul, Syamimi Saadon, and Mohd Hasrizam Che Man. "Heat Transfer Enhancement of Biomass Based Stirling Engine." *Journal of Advanced Research in Fluid Mechanics and Thermal Sciences* 100, no. 1 (2022): 1-10. <https://doi.org/10.37934/arfmts.100.1.110>
- [28] Cardozo, Evelyn, Catharina Erlich, Anders Malmquist, and Lucio Alejo. "Integration of a wood pellet burner and a Stirling engine to produce residential heat and power." *Applied Thermal Engineering* 73, no. 1 (2014): 671-680. <https://doi.org/10.1016/j.applthermaleng.2014.08.024>
- [29] Jufrizal, Jufrizal, Farel H. Napitupulu, Ilmi Ilmi, and Himsar Ambarita. "Manufacturing and testing prototype of a gamma type Stirling engine for micro-CHP application." In *IOP Conference Series: Materials Science and Engineering*, vol. 725, no. 1, p. 012016. IOP Publishing, 2020. <https://doi.org/10.1088/1757-899X/725/1/012016>
- [30] Jufrizal, Jufrizal, Farel H. Napitupulu, Ilmi Ilmi, Himsar Ambarita and Mahadi Meliala. "Thermodynamic Analysis of a Gamma-Type Stirling Engine for mCHP Application." In *Proceedings of the 7th International Conference and Exhibition on Sustainable Energy and Advanced Materials (ICE-SEAM 2021)*, Melaka, Malaysia, p. 225. Springer Nature, 2022. https://doi.org/10.1007/978-981-19-3179-6_40
- [31] Jufrizal, Jufrizal, Farel H. Napitupulu, Ilmi Ilmi, Himsar Ambarita and Mahadi Meliala. "Ideal Cycle Thermodynamic Analysis for Gamma-Type Stirling Engine." *Journal of Mechanical Engineering and Technology (JMETS)* 14, no. 2 (2022): 1-15. https://doi.org/10.1007/978-981-19-3179-6_40

- [32] Ferral-Smith, Hayden, Georgia Giannakakis, Joshua Wilson, and Joshua Taylor. "Factors Influencing the Thermodynamic Efficiency of Stirling Engines." *PAM Review Energy Science & Technology* 4 (2017): 17-29. <https://doi.org/10.5130/pamr.v4i0.1459>
- [33] Abuelyamen, Ahmed, and Rached Ben-Mansour. "Energy efficiency comparison of Stirling engine types (α , β , and γ) using detailed CFD modeling." *International Journal of Thermal Sciences* 132 (2018): 411-423. <https://doi.org/10.1016/j.ijthermalsci.2018.06.026>
- [34] Ahmadi, Mohammad H., Mohammad-Ali Ahmadi, and Fathollah Pourfayaz. "Thermal models for analysis of performance of Stirling engine: A review." *Renewable and Sustainable Energy Reviews* 68 (2017): 168-184. <https://doi.org/10.1016/j.rser.2016.09.033>
- [35] Mukhtar, Munir Afnan, Rosli Abu Bakar, and Mohd Farid Zainudin. "Thermodynamic Analysis of a Gamma-configuration Stirling Engine." *Journal of Advanced Research in Fluid Mechanics and Thermal Sciences* 83, no. 2 (2021): 114-126. <https://doi.org/10.37934/arfmts.83.2.114126>
- [36] Kusnandar, Nanang. "Metode pengukuran asupan panas kompor gas berdasarkan SNI 7638: 2011 dan SNI 7469: 2013." *Jurnal Standardisasi* 17, no. 3 (2016): 233-240. <https://doi.org/10.31153/js.v17i3.323>
- [37] Ambarita, Himsar, Eko Yohanes Setyawan, Sibuk Ginting, and Waldemar Naibaho. "Performance of a small compression ignition engine fuelled by liquified petroleum gas." In *IOP Conference Series: Materials Science and Engineering*, vol. 237, no. 1, p. 012011. IOP Publishing, 2017. <https://doi.org/10.1088/1757-899X/237/1/012011>
- [38] Islam, Ashfarul, Hridoy Roy, and Md Mominur Rahman. "Energy efficiency study of household natural gas burner using pot-bottom shield and modified pot arrangement." *Energy Reports* 8 (2022): 12871-12885. <https://doi.org/10.1016/j.egy.2022.09.136>
- [39] Cengel, Yunus A., and Michael A. Boles. *Thermodynamics: an engineering approach*. McGraw-Hill Higher Education, 2006.
- [40] Shen, Guofeng, Michael D. Hays, Kirk R. Smith, Craig Williams, Jerroll W. Faircloth, and James J. Jetter. "Evaluating the performance of household liquefied petroleum gas cookstoves." *Environmental Science & Technology* 52, no. 2 (2018): 904-915. <https://doi.org/10.1021/acs.est.7b05155>
- [41] Alfarawi, Suliman, Raya Al-Dadah, and Saad Mahmoud. "Influence of phase angle and dead volume on gamma-type Stirling engine power using CFD simulation." *Energy Conversion and Management* 124 (2016): 130-140. <https://doi.org/10.1016/j.enconman.2016.07.016>